

Artikel 1_1

by Ariswan Ariswan

Submission date: 29-Apr-2019 08:55PM (UTC+0700)

Submission ID: 1121325038

File name: Artikel_1_1.pdf (866.73K)

Word count: 3104

Character count: 14843

1
PHYSICOCHEMICAL PROPERTIES OF Sn(S_{1-x}Te_x) SOLID SOLUTIONS OF BOTH MASSIVE MATERIALS AND THIN FILMSA. ARISWAN^{a*}, R. PRASETYOWATI^a, H. SUTRISNO^b^a*Department of Physics Education, Faculty of Mathematics and Natural Sciences, University Negeri Yogyakarta, Yogyakarta 55281, Indonesia*^b*Department of Chemistry Education, Faculty of Mathematics and Natural Sciences, University Negeri Yogyakarta, Yogyakarta 55281, Indonesia*

The Sn(S_{1-x}Te_x) solid solutions have been prepared on both massive materials and thin films with variation of x value of 0, 0.2, 0.4, 0.6, 0.8, and 1.0. The massive materials were prepared by Bridgman technique, while the thin films were obtained with vacuum evaporation technique. Phase and crystal structure of both massive materials and thin films were investigated by X-ray diffraction (XRD). The chemical compositions were determined by energy dispersive X-ray spectroscopy (EDAX). Especially for thin films, the surface morphology was studied by scanning electron microscopy (SEM), while the optical properties were obtained by UV-Vis-NIR spectrophotometers. The results show that the crystalline structures of all materials have an orthorhombic structure when dominated by sulfur atom, while having a cubic structure for tellurium atom dominance. All samples are p-type semiconductors and the optical properties show a reduction of the band gaps when the tellurium atomic composition increases.

(Received January 8, 2018; Accepted March 22, 2018)

Keywords: Bridgman technique, Vacuum evaporation techniques, Solid solutions**1. Introduction**

15

Tin chalcogenide nanoparticles, SnS and SnTe have received considerable attention because of their interesting optoelectronic properties. Tin monosulfide (SnS) is p-type semiconductor that attract the attention of the researchers in the context of photovoltaic conversion. Bulk SnS has both a direct band gap ($E_{g,dir} = 1.32$ eV) and indirect band gap ($E_{g,ind} = 1.08$ eV) [1, 2], which is very close to that of silicon and is especially attractive due to its high conversion efficiency in photovoltaic devices (~25%) [3]. The efforts to produce new photovoltaic materials with high efficiency are needed because each country will experience a conventional energy crisis as well as the pollution issue it generates. Crystal of SnS crystallizes in the orthorhombic structure of space group *Pbmm* [4, 5]. The SnS is of crystallographic interest because it is intermediate between three-dimensional crystalline networks and two-dimensional layer type compounds [6]. Tin telluride (SnTe) is an important narrow band gap semiconductor material. Bulk SnTe is a semiconductor with a direct band gap of 0.35 eV [7-9], which is narrower than that of the bulk SnS. Kovalenko et al. (2007) report a solution-phase synthesis of high-quality colloidal SnTe nanocrystals with mean diameters tunable in the range of ca. 4.5-15 nm and corresponding band gaps of 0.80- 0.38 eV [10]. At room temperature, crystal of SnTe crystallizes in the cubic structure of space group *Fm-3m* [11].

The doping tellurium (Te) on SnS is expected to reduce band gap of SnS so that obtained material with band gap in accordance with maximum theoretical conversion efficiency in solar cell [12]. In this paper, we report the preparation of Sn(S_{1-x}Te_x) bulks by Bridgman technique and Sn(S_{1-x}Te_x) thin films by vacuum evaporation techniques. Therefore, this study specifically aims to determine the effect of atom fraction of Te on SnS. The effect is estimated on two important points. First, it relates in the crystal structure (lattice parameter). This point corresponds to the

*Corresponding author: ariswan@uny.ac.id

dependence of the $\text{Sn}(\text{S}_{1-x}\text{Te}_x)$ lattice parameter to the tellurium atom x fraction. Secondly, it relates to the band gap width dependence as a function of the fraction x of the tellurium atom. These two physical quantities are very important in relation to the p-n junction of solar cells, especially in the ability of material absorption to solar energy. The optical and structural properties of the $\text{Sn}(\text{S}_{1-x}\text{Te}_x)$ solid solutions have been investigated on both massive materials and thin films. Its were studied using UV-Vis-NIR spectrophotometer, X-ray diffraction (XRD), scanning electron microscopy (SEM), and energy dispersive of X-ray spectroscopy (EDAX).

2. Experimental

2.1. Sample Preparation

The materials needed for the preparation of massive materials of solid solution are tin (Sn), sulfur (S) and tellurium (Te). Each material has a degree of purity 99.99%. The study was distinguished in three steps. First step, preparation of bulks of $\text{Sn}(\text{S}_{1-x}\text{Te}_x)$ solid solutions using Bridgman technique. For the preparation of $\text{Sn}(\text{S}_{1-x}\text{Te}_x)$, first weighed tin (Sn) eg. p gram. Further calculated sulfur mass S using the following formula: $\left(\frac{p}{(BA)_{\text{Sn}}}(1-x)(BA)_{\text{S}}\right)$ gram, while the mass of tellurium (Te) can be calculated by the formula: $\left(\frac{p}{(BA)_{\text{Sn}}}(x)(BA)_{\text{Te}}\right)$ gram, where, BA denotes the atomic weight. Furthermore, the three metal materials: Sn, S and Te are inserted in pyrex tubes having an inner and outer diameter of 12 and 16 mm, respectively. The tubes were previously washed with a mixture of HF, HNO_3 and H_2O solutions with a ratio of 2: 3: 5 and dried in a heating chamber at 80°C for 8 hours. The tube containing the above materials was placed on a 10^{-5} Torr vacuum and welded at one end, resulting in a capsule containing: Sn, S and Te. The capsule was then placed in a furnace whose temperature and duration of maintaining the temperature can be adjusted as required in the form of a heating flow. The second step, thin films were reproduced using vacuum evaporation techniques. The evaporator reactor system was made of 30 cm diameter quartz tube placed over a vacuum system comprising a primary pump and a secondary pump. As the source or target was a solid solution of $\text{Sn}(\text{S}_{1-x}\text{Te}_x)$ prepared by Bridgman technique which was then crushed so as to form powder. The powder was placed on a boat-based heating source that can be heated to a temperature above 1500°C made of molybdenum (Mo) material. The temperature of the cup was measured using a thermocouple. Between source and substrate separated by a separator whose distance can be varied at 10, 15, and 25 cm. Meanwhile around the substrate was installed substrate heating due to crystallization of the thin layer will occur with substrate temperature above 300°C [13]. The advantage of this technique was that the thin film yields the same composition and structure as the source of the massive solid solution target and the working pressure of 10^{-5} Torr, thus using primary and secondary pumps or diffusion pumps.

2.2. Sample Characterization

The chemical compositions of massive materials and thin films of $\text{Sn}(\text{S}_{1-x}\text{Te}_x)$ were determined by energy dispersive X-ray spectroscopy (EDAX) from EDAX Inc., while the surface morphology of thin films were investigated by scanning electron microscopy (SEM) (Jeol JSM-6360). The machine was operated at an acceleration voltage of 20 keV at a working distance of 10 mm to identify the morphological properties of samples.

The prepared samples were examined for the investigation of phase and structure using a Rigaku Miniflex 600-benchtop X-ray Diffraction (XRD), operated in the Bragg configuration using $\text{Cu K}\alpha$ radiation ($\lambda = 1.5406 \text{ \AA}$). The intensities were determined in the 2θ collection range of 20° to 90° . The XRD instrument was run at 40 kV and 15 mA. The lattice parameters and Bravais lattice from the powder diffraction data were carried out using least squares refinement method by the U-fit program [14].

Ultra violet-visible (UV-Vis) absorption measurements of thin film samples were performed by UV-Vis spectrophotometers (Shimadzu, UV-2600) in the wavelength range of 200-900 nm. The absorption coefficient α on UV-VIS spectroscopy satisfies the following equation [15]:

12

$$\alpha \cdot hv = B (hv - E_g)^n$$

where h is Planck's constant (6.626×10^{-34} Js), v is the wave frequency (Hz), B is a constant of 10^5 to 10^6 , while n is $\frac{1}{2}$ for direct band gap, where n is 1 for indirect transitions, hv is the energy of photons in electron volt (eV), E_g is the band gap or energy gap (eV). The band gap can be determined by performing absorbance data analysis that is the relationship with absorbance coefficient A with the absorption coefficient α . The relationship of both is linear, whereas in semiconductor materials apply the equation as mentioned above with $n = \frac{1}{2}$. The band gap value (E_g) can be determined which is the value when the left side is equal to zero:

$$(\alpha \cdot hv)^2 = B^2 (hv - E_g)$$

24

3. Results and discussion

3.1. SEM and EDAX

EDAX characterization is performed on both a massive sample and a thin film. Table 1 shows the chemical composition of massive materials of $\text{Sn}(\text{S}_{1-x}\text{Te}_x)$ solid solutions and the thin film as shown in the Table 2. The EDAX results show the compatibility of chemical composition between massive material and thin film. This shows the superiority of vacuum evaporation techniques.

Table 1. Chemical composition of $\text{Sn}(\text{S}_{1-x}\text{Te}_x)$ massive materials

| Solid Solutions Expected | Chemical Composition (wt %) | | | Solid Solutions Obtained |
|--|-----------------------------|-------|--------|--|
| | Sn (%) | S (%) | Te (%) | |
| SnS | 52.79 | 47.15 | - | $\text{SnS}_{0.89}$ |
| $\text{Sn}(\text{S}_{0.80}\text{Te}_{0.20})$ | 53.27 | 37.67 | 9.06 | $\text{Sn}(\text{S}_{0.71}\text{Te}_{0.17})$ |
| $\text{Sn}(\text{S}_{0.60}\text{Te}_{0.40})$ | 50.26 | 28.26 | 20.88 | $\text{Sn}(\text{S}_{0.56}\text{Te}_{0.44})$ |
| $\text{Sn}(\text{S}_{0.40}\text{Te}_{0.60})$ | 50.86 | 11.94 | 37.19 | $\text{Sn}(\text{S}_{0.20}\text{Te}_{0.70})$ |
| $\text{Sn}(\text{S}_{0.20}\text{Te}_{0.80})$ | 46.86 | 9.08 | 44.06 | $\text{Sn}(\text{S}_{0.19}\text{Te}_{0.94})$ |
| SnTe | 53.6 | - | 46.95 | $\text{SnTe}_{0.88}$ |

Table 2. Chemical compositions of $\text{Sn}(\text{S}_{1-x}\text{Te}_x)$ thin films

| Solid Solutions Expected | Chemical Composition (wt %) | | | Solid Solutions Obtained |
|--|-----------------------------|-------|--------|--|
| | Sn (%) | S (%) | Te (%) | |
| SnS | 55.00 | 45.00 | - | $\text{SnS}_{0.80}$ |
| $\text{Sn}(\text{S}_{0.80}\text{Te}_{0.20})$ | 51.20 | 40.41 | 8.39 | $\text{Sn}(\text{S}_{0.79}\text{Te}_{0.16})$ |
| $\text{Sn}(\text{S}_{0.60}\text{Te}_{0.40})$ | 51.87 | 28.41 | 19.72 | $\text{Sn}(\text{S}_{0.55}\text{Te}_{0.38})$ |
| $\text{Sn}(\text{S}_{0.40}\text{Te}_{0.60})$ | 54.54 | 10.85 | 34.61 | $\text{Sn}(\text{S}_{0.18}\text{Te}_{0.64})$ |
| $\text{Sn}(\text{S}_{0.20}\text{Te}_{0.80})$ | 52.31 | 0.88 | 46.81 | $\text{Sn}(\text{S}_{0.02}\text{Te}_{0.89})$ |
| SnTe | 51.92 | - | 49.08 | $\text{SnTe}_{0.94}$ |

20

The surface morphology of thin films was investigated by SEM. Figure 1 show SEM images of $\text{Sn}(\text{S}_{1-x}\text{Te}_x)$ thin films. SEM images show that the surface structures of thin films with sulfur and tellurium dominant are significantly different. The first surface of Fig. 1(a), 1(b), and 1(c) related to the orthorhombic structures. The second surface of Fig. 1(d), 1(e) and 1(f) looks related to the cubic structures.

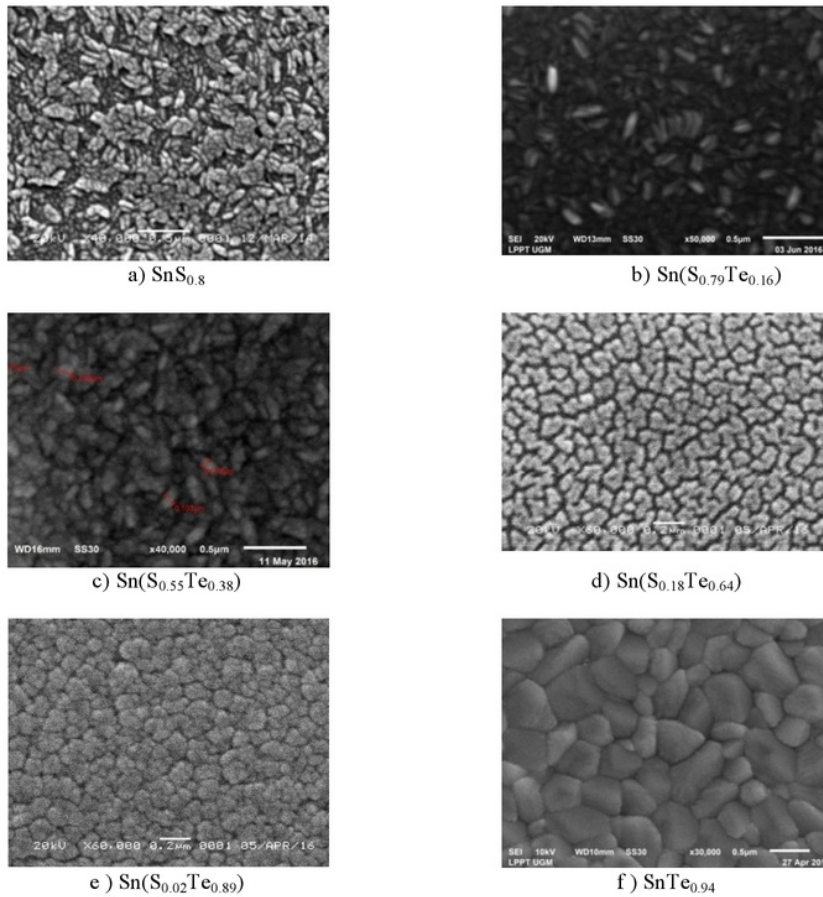
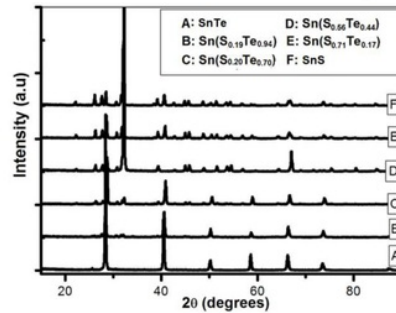


Fig. 1. SEM images of $\text{Sn}(\text{S}_{1-x}\text{Te}_x)$ thin films

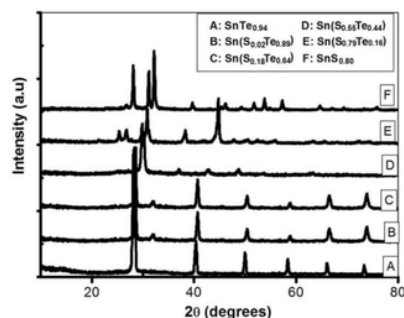
3.2. Structural Characterization

Fig. 2 and 3 depict the XRD patterns of $\text{Sn}(\text{S}_{1-x}\text{Te}_x)$ solid solutions of massive materials and thin films, respectively. The XRD patterns were recorded in 2θ range of $15\text{--}90^\circ$. These diffraction peaks are consistent with the reflections of SnS phase and SnTe. The XRD results of tin monosulfide (SnS) and tin monotelluride (SnTe) are completely different characteristics.



32

Fig. 2. XRD patterns of $\text{Sn}(\text{S}_{1-x}\text{Te}_x)$ massive materials



30
Fig. 3. XRD patterns of $\text{Sn}(\text{S}_{1-x}\text{Te}_x)$ thin films

X-ray diffraction pattern shows the peaks that appear in the sample. XRD results data obtained from the research sample. The crystal lattice parameters (a, b and c) formed can be calculated by least squares refinement method [14]. The calculation results show that the crystal structure of SnS is orthorhombic, while the SnTe is cubic with lattice parameters as in Table 3. The massive materials and thin films of $\text{Sn}(\text{S}_{1-x}\text{Te}_x)$ solid solutions have the same structure. The crystal structure in the thin films is orthorhombic when the dominance of sulfur atoms, and will become cubic structure when the dominance of tellurium atoms. X-ray diffraction peaks of SnS represent orthorhombic structures with space group $Pbnm$, whereas SnTe is related to cubic structures with space group $Fm-3m$. The peaks of the X-ray diffractogram emerging from the SnS and SnTe crystals relate to crystalline planes (hkl) or Miller indices. For SnS crystals, the emerging peaks are as diverse as peaks (111) corresponding to 2θ at 31.8° , while for SnTe crystals, the highest peak at an angle of 29.71° indicates the crystalline planes (200). Overall, the peaks appearing on the SnTe crystals represent the cubic structure with the bravais lattice of the center cubic. The result of calculation of lattice parameters of each $\text{Sn}(\text{S}_{1-x}\text{Te}_x)$ solid solutions of both massive materials and thin films can be given in Table 3.

Table 3. Lattice parameters of both massive materials and thin films of $\text{Sn}(\text{S}_{1-x}\text{Te}_x)$ solid solutions

| $\text{Sn}(\text{S}_{1-x}\text{Te}_x)$ Solid Solutions | Massive Materials | | | Crystal System | Figure of Merit | |
|--|-------------------|--------|-------|------------------------------|-----------------|-------|
| | a (Å) | b (Å) | c (Å) | | D | R |
| SnS | 4.317 | 11.447 | 3.895 | Orthorhombic, $Pbnm$ | 0.022 | 0.025 |
| $\text{Sn}(\text{S}_{0.71}\text{Te}_{0.17})$ | 4.329 | 11.196 | 3.984 | Orthorhombic, $Pbnm$ (major) | 0.032 | 0.051 |
| $\text{Sn}(\text{S}_{0.56}\text{Te}_{0.44})$ | 4.337 | 11.205 | 3.991 | Orthorhombic, $Pbnm$ (major) | 0.027 | 0.039 |
| $\text{Sn}(\text{S}_{0.20}\text{Te}_{0.70})$ | 6.319 | 6.319 | 6.319 | Cubic, $Fm-3m$ (major) | 0.009 | 0.030 |
| $\text{Sn}(\text{S}_{0.19}\text{Te}_{0.94})$ | 6.320 | 6.320 | 6.320 | Cubic, $Fm-3m$ (major) | 0.013 | 0.027 |
| SnTe | 6.322 | 6.322 | 6.322 | Cubic, $Fm-3m$ | 0.042 | 0.056 |
| Thin Films | | | | | | |
| $\text{SnS}_{0.80}$ | 4.293 | 11.217 | 3.910 | Orthorhombic, $Pbnm$ | 0.028 | 0.031 |
| $\text{Sn}(\text{S}_{0.79}\text{Te}_{0.16})$ | 4.286 | 11.118 | 3.946 | Orthorhombic, $Pbnm$ (major) | 0.021 | 0.031 |
| $\text{Sn}(\text{S}_{0.55}\text{Te}_{0.38})$ | 4.230 | 11.190 | 4.030 | Orthorhombic, $Pbnm$ (major) | 0.042 | 0.053 |
| $\text{Sn}(\text{S}_{0.18}\text{Te}_{0.64})$ | 6.303 | 6.303 | 6.303 | Cubic, $Fm-3m$ (major) | 0.031 | 0.068 |
| $\text{Sn}(\text{S}_{0.02}\text{Te}_{0.89})$ | 6.304 | 6.304 | 6.304 | Cubic, $Fm-3m$ (major) | 0.044 | 0.062 |
| $\text{SnTe}_{0.94}$ | 6.309 | 6.309 | 6.309 | Cubic, $Fm-3m$ | 0.063 | 0.092 |

The characteristic factors of the refinement (D) are the mean deviation between $2\theta_{\text{obs}}$ and $2\theta_{\text{calc}}$, that is $D = \frac{1}{n_{\text{hkl}}} \sum |d(2\theta)|$ and the confidence factor (R) given by the following relation: $R = \frac{1}{n_{\text{hkl}} - n_{\text{var}}} \sum (2\theta_{\text{obs}} - 2\theta_{\text{calc}})^2$, where n_{hkl} is the number of reflections taken into account and n_{var} is the number of refined variables

3.3. Optical Properties

The result of UV-VIS in absorbance form as a photon wave function can be shown in Figure 4. Figure 4 shows that the absorbance is highly dependent on the material band gap. When the photon comes with the photon energy smaller than the band gap material then there is almost no photon uptake by the material. Furthermore, when the photon energy is the same as the band gap then there is a very drastic change that is the appearance of photon uptake by the material. A special case in this sample is that the photon energy range between the wavelengths of 200 nm to 800 nm or the energy range from 1.5 eV to 6.2 eV.

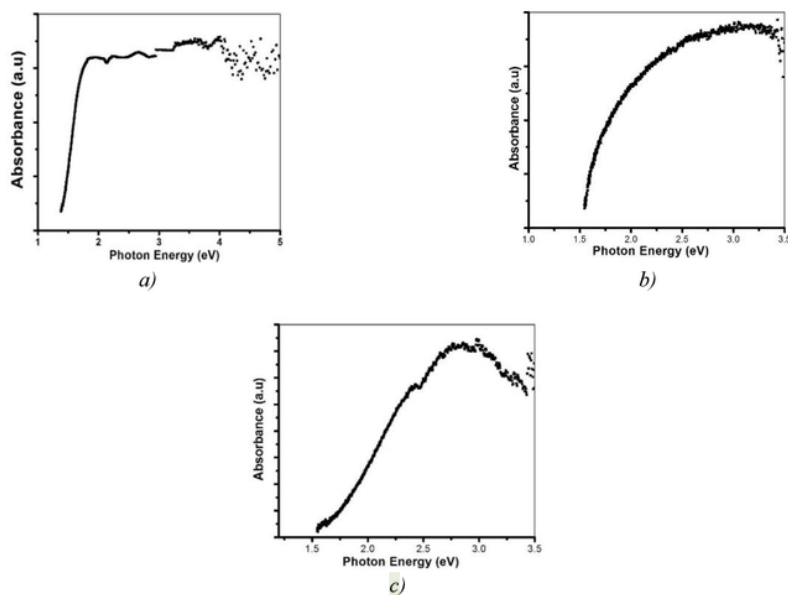


Fig. 4. Absorbance on a thin layer of (a). SnS , (b). $\text{Sn}(\text{S}_{0.8}\text{Te}_{0.2})$ and (c). $\text{Sn}(\text{S}_{0.6}\text{Te}_{0.4})$

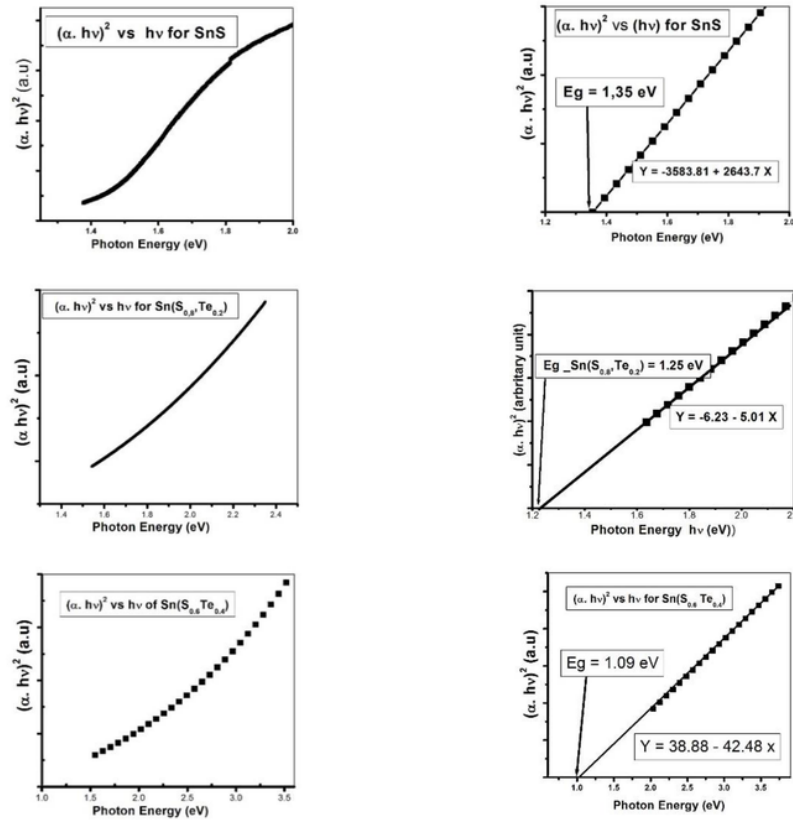


Fig. 5. Graph $(\alpha \cdot hv)^2$ as a function of photon energy hv of $Sn(S_{1-x}Te_x)$

The first SnS has a 1.35 eV band gap, while SnTe has a 0.4 eV band gap, so it is believed that Sn(S,Te) has a band gap between 1.35 eV and 0.3 eV. The determination can be shown in the Figure 5. According to Figure 5, the energy gap SnS is obtained at 1.35 eV and decreases to 1.25 eV when there is a tellurium fraction of 20%. The band gap decreases again when the atomic fraction of Te gets larger by 1.09 eV for Te fraction to 40%.

4. Conclusions

The results of the research show the crystal structure and lattice parameters (a, b and c) of massive materials and thin films of the $Sn(S_{1-x}Te_x)$ depends on the dominance of the constituent atoms both sulfur and tellurium atoms. The situation is generally applicable to both massive materials and thin films. If the majority of the constituents are Te atoms then the solid solutions and thin films have a cubic structure whereas if dominance by sulfur atoms then it has an orthorhombic crystal structure. The measurement of the chemical composition of the entire sample preparation is non-stoichiometry which presents a deviation from the hope atomic composition, but in reality the third phase of the atom is already formed in both a massive solid solution and a thin film. The surface morphology shows the grain size indicating the formation of crystals in each of the preparation results on massive material and thin film according to the reality of XRD results. Measurement of all electric properties of $Sn(S_{1-x}Te_x)$ has a p-type conductivity with

resistance in accordance with semiconductor material. The band gap decreases as Te atomic fraction increases.

4

Acknowledgements

The authors gratefully acknowledge the financial support of Ministry of Research, Technology and Higher Education of the Republic of Indonesia based on Hibah Bersaing Grant, No. 51/Penel./P.Produk Terapan/UN34.21/2017.

References

- [1] W. Albers, C. Haas, H.J. Vink, H. J. D. Wasscher, *J. Appl. Phys.* **32**, 2220 (1961).
- [2] O. E. Ogah, G. Zoppi, I. Forbes, R. W. Miles, 23rd European Photovoltaics Solar Energy Conference, p.2580 (Sept. 2008).
- [3] J. P. Singh, R. K. Bedi, *Thin Solid Films* **199**, 9 (1991).
- [4] B. B. Nariya, A. K. Dasadia, M. K. Bhayani, A. J. Patel, A. R. Jani, *Chalcogenide Letters* **6**(10), 549 (2009).
- [5] P. S. del Bucchia, J. C. Jumas, M. Maurin, *Acta Crystallogr.* **B37**, 1903 (1981).
- [6] Logothetidis, S.; Polatoglou, H. M. *Phys. Rev. B* **36**, 7491 (1987).
- [7] A. Ishida, T. Tsuchiya, Takaoka, *AIP Conf. Proc.* **1399**, 127 (2011).
- [8] A. Aggarwal, P. D. Patel, D. Lakshminarayana, *J. Crys. Growth* **142**, 344 (1994).
- [9] R Saini, Pallavi, M. Singh, R. Kumar, G. Jain, *Chalcogenide Letters* **7**(3), 197 (2010).
- [10] M. V. Kovalenko, W. Heiss, E. V. Shevchenko, J. S. Lee, H. Schwinghammer, A. P. Alivisatos, D. V. Talapin, *J. Am. Chem. Soc.* **129**, 11354 (2007).
- [11] Landolt-Bornstein, Springer-Verlag: Berlin, Vol. 17 (1983).
- [12] A. Goetzberger, C. Hebling, *Solar Energy Materials and Solar Cells* **62**, 1 (2000).
- [13] A. Zouaoui, M. Lachab, M. L. Hidalgo, A. Chaffa, C. Linares, N. Kesri, *Thin Solid Films* **339**, 10 (1999).
- [14] M. Evain, U-FIT: A cell parameter refinement program, IMN Nantes, France, (1992).
- [15] H. Sakata, H. Ogawa, *Solar Energy Materials and Solar Cells* **63**, 259 (2000).

Artikel 1_1

ORIGINALITY REPORT

19%

SIMILARITY INDEX

8%

INTERNET SOURCES

16%

PUBLICATIONS

4%

STUDENT PAPERS

PRIMARY SOURCES

- 1 Anggraeni Kumala Dewi, Ariswan. "The Characterization of Semiconductor Crystal Sn($\text{Se}_{0.8}\text{Te}_{0.2}$) Prepared by Bridgman Technique for Solar Cell", Materials Science Forum, 2019
Publication 3%
- 2 Yingyot Infahsaeng, Sarute Ummartyotin. "Investigation on structural properties of Al-substituted ZnS particle prepared from wet chemical synthetic route", Results in Physics, 2017
Publication 2%
- 3 pubs.acs.org
Internet Source 2%
- 4 www.nanosmat.co.uk
Internet Source 1%
- 5 Philip Boudjouk, Dean J. Seidler, Dean Grier, Gregory J. McCarthy. "Benzyl-Substituted Tin Chalcogenides. Efficient Single-Source Precursors for Tin Sulfide, Tin Selenide, and

Sn(S Se) Solid Solutions ", Chemistry of Materials, 1996

Publication

| | | |
|----|--|----|
| 6 | www.scientific.net Internet Source | 1% |
| 7 | Submitted to Universitas Islam Indonesia Student Paper | 1% |
| 8 | Dyah Purwaningsih, Roto Roto, Hari Sutrisno, Agus Purwanto. "Structural characterization of $\text{LiCr}_x\text{Mn}_{2-x}\text{O}_4$ via a simple reflux technique", AIP Publishing, 2017 Publication | 1% |
| 9 | Submitted to School of Business and Management ITB Student Paper | 1% |
| 10 | R.K. Saini, R. Kumar, Garima Jain. "Optical studies of $\text{SnTe}_x\text{Se}_{1-x}$ sintered films", Optical Materials, 2009 Publication | 1% |
| 11 | Environmental Science and Engineering, 2014. Publication | 1% |
| 12 | kuislide.com Internet Source | 1% |
| 13 | www.springerprofessional.de Internet Source | 1% |

14

sig3.ecanews.org

Internet Source

1%

15

Ying Xu, Najeh Al-Salim, Justin M. Hodgkiss, Richard D. Tilley. "Solution Synthesis and Optical Properties of SnTe Nanocrystals", *Crystal Growth & Design*, 2011

Publication

1%

16

Priscilla D. Antunez, Daniel A. Torelli, Fan Yang, Federico A. Rabuffetti, Nathan S. Lewis, Richard L. Brutchey. "Low Temperature Solution-Phase Deposition of SnS Thin Films", *Chemistry of Materials*, 2014

Publication

1%

17

Mohammad Javad Jafari. "Effect of chemical environments on palladium phthalocyanine thin film sensors for humidity analysis", *Journal of Materials Science*, 10/04/2011

Publication

<1%

18

Purwaningsih, D, R Roto, and H Sutrisno. "Synthesis of $\text{LiNi}_x\text{Mn}_{2-x}\text{O}_4$ by low-temperature solid-state reaction and its microstructure", *IOP Conference Series Materials Science and Engineering*, 2016.

Publication

<1%

19

eprints.uny.ac.id

Internet Source

<1%

| | | |
|----|---|-----|
| 20 | doaj.org Internet Source | <1% |
| 21 | Hyeongsu Choi, Jeongsu Lee, Seokyeon Shin, Juhyun Lee et al. " Fabrication of high crystalline SnS and SnS thin films, and their switching device characteristics ", Nanotechnology, 2018 Publication | <1% |
| 22 | www.eeel.nist.gov Internet Source | <1% |
| 23 | nagoya.repo.nii.ac.jp Internet Source | <1% |
| 24 | Chen, Cheng-Lung, Heng Wang, Yang-Yuan Chen, Tristan Day, and G. Jeffrey Snyder. "Thermoelectric properties of p-type polycrystalline SnSe doped with Ag", Journal of Materials Chemistry A, 2014. Publication | <1% |
| 25 | Beta Wulan Febriana, Widinda Normalia Arlianty, Artina Diniaty. "Scientific method by using project method in acid, base and salt material", AIP Publishing, 2017 Publication | <1% |
| 26 | Satish Gupta. "Symmetry systematics of pressure - induced phase transitions", High Pressure Research, 5/1/1994 | <1% |

27

Submitted to Universiti Sains Malaysia

Student Paper

<1%

28

R. E. Banai, L. A. Burton, S. G. Choi, F. Hofherr, T. Sorgenfrei, A. Walsh, B. To, A. Cröll, J. R. S. Brownson. " Ellipsometric characterization and density-functional theory analysis of anisotropic optical properties of single-crystal - SnS ", Journal of Applied Physics, 2014

Publication

<1%

29

chemweb.com

Internet Source

<1%

30

Song, Jae Yong. "Layered intermetallic compounds and stress evolution in Sn and Ni(P) films", Journal of Materials Research, 2007.

Publication

<1%

31

Koteeswara Reddy, N., M. Devika, and E. S. R. Gopal. "Review on Tin (II) Sulfide (SnS) Material: Synthesis, Properties, and Applications", Critical Reviews in Solid State and Material Sciences, 2015.

Publication

<1%

32

Liu, Moumiao, Wenchao Yang, Yueyuan Ma, Chenghuang Tang, Hongqun Tang, and Yongzhong Zhan. "The electrochemical

<1%

corrosion behavior of Pb-free Sn-8.5Zn-XCr
solders in 3.5 wt.% NaCl solution", Materials
Chemistry and Physics, 2015.

Publication

Exclude quotes On

Exclude matches < 2 words

Exclude bibliography On

Artikel 1_1

GRADEMARK REPORT

FINAL GRADE

/100

GENERAL COMMENTS

Instructor

PAGE 1

PAGE 2

PAGE 3

PAGE 4

PAGE 5

PAGE 6

PAGE 7

PAGE 8
